Received: 28 May 2024 | Revised: 9 October 2024 | Accepted: 9 October 2024

DOI: 10.1111/iwj.70108

ORIGINAL ARTICLE

IWJ WILEY

Comparison of cell-scaffold interactions in a biological and a synthetic wound matrix

Joon Pio Hong[1] | **Joanneke Maitz**[2,3] | **Matthias Mörgelin**[4]

[1]Department of Plastic Surgery, Asan Medical Center, University of Ulsan, Ulsan, South Korea

[2]Burns & Reconstructive Surgery Research Group, ANZAC Research Institute, Concord Hospital, Sydney, Australia

[3]Faculty of Medicine & Health, University of Sydney, Sydney, Australia

[4]Colzyx AB, Medicon Village, Lund, Sweden

Correspondence
Matthias Mörgelin, Colzyx AB, Medicon Village, SE-223 81 Lund, Sweden.
Email: matthias@colzyx.com

Abstract

Wound healing is a central physiological process that restores the barrier properties of the skin after injury, comprising close coordination between several cell types (including fibroblasts and macrophages) in the wound bed. The complex mechanisms involved are executed and regulated by an equally complex, reciprocal signalling network involving numerous signalling molecules such as catabolic and anabolic inflammatory mediators (e.g., cytokines, chemokines). In chronic wound environments, the balance in the molecular signatures of inflammatory mediators is usually impaired. Thus, we compared the ability of a collagen-based wound matrix against a synthetic wound matrix to attract fibroblasts and macrophages that deliver these signalling molecules. In particular, the balance between pro- and anti- inflammatory cytokine secretion was assessed. We found that the natural collagen-based matrix was the most efficient adhesive substrate to recruit and activate fibroblasts and macrophages on its surface. These cells secreted a variety of cytokines, and the natural biomaterial exhibited a more balanced secretion of pro- and anti-inflammatory mediators than the synthetic comparator. Thus, our study highlights the ability of native collagen matrices to modulate inflammatory mediator signatures in the wound bed, indicating that such devices may be beneficial for wound healing in the clinical setting.

KEYWORDS

extracellular matrix, fibrillar collagens, inflammation mediators, tissue scaffolds, wound healing

Key Messages

- Wound healing depends on close coordination between several cell types (including fibroblasts and macrophages) and signalling molecules (e.g., catabolic and anabolic inflammatory mediators) in the wound bed.

- We assessed a biological collagen matrix and its potential to act as adhesive substrate for fibroblasts and macrophages, compared with a synthetic wound matrix.
- We found that fibroblasts and macrophages adhere, survive and proliferate more rapidly using the biological collagen matrix compared with the synthetic comparator.
- The ratio between secretion of pro- and anti-inflammatory cytokines was also more balanced on the biological collagen matrix.
- Thus, a biological collagen matrix may be beneficial for wound management in clinical practice by enabling fibroblasts and macrophages to proliferate and modulating the molecular signatures of catabolic and anabolic inflammatory mediators in the wound environment.

1 | INTRODUCTION

After an injury, the integrity of skin is restored via multicellular, complex and interconnected physiological processes.[1] Devitalized tissue is replaced over a period of time with neo-tissue in highly regulated and dynamic events, including coagulation, formation of granulated tissue, re-epithelialization and remodelling of the extracellular matrix.[2] The resultant migration, infiltration, proliferation and differentiation of different cell types (e.g., keratinocytes, fibroblasts, endothelial cells, macrophages, platelets) in symbiosis with an inflammatory response is essential to normal wound healing, culminating in the formation of new tissue to achieve wound closure.[3–5]

Although this sequence of events occurs in most wounds, the complexity of wound healing, combined with underlying co-morbidities, such as diabetes, increases susceptibility to a malfunction in any of the processes involved. When this happens, wound healing breaks down, leading to a chronic wound environment and delayed wound healing.[6] Chronic wounds are characterized by a damaged extracellular matrix and impaired new tissue formation in the wound bed, accompanied by abnormal inflammation that disrupts the normal healing cascade.[7] This pathological inflammation is mainly governed by an impaired balance in the intercellular communication between resident leucocytes and skin cells in the wound bed that is dependent on signalling molecules such as growth factors, cytokines and chemokines.[8,9] The impairment in these molecular signatures reflects a reduced capacity to synthesize new tissue and the antagonistic activities of high levels of proteinases within the chronic wound bed.[1]

To aid the host in its tissue repair, scaffolds have been designed to promote cellular migration and restoration of the extracellular dermal matrix. Since its inception in 1975 when the pioneers Yannas and Burke developed the first artificial dermis in the form of a bovine collagen matrix, advances in biomaterials and the processing of biomaterials have been made that has led to a wide array of commercially available dermal templates.[10,11] The new generation of devices being tested are designed to actively interact with the wound and drive tissue regeneration. One of the key features to drive tissue regeneration is defined by scaffold–cell interaction. Integration of host cells into the matrix stimulates neo-dermal regeneration over which keratinocytes can re-epithelialize the wound effectively. The biomaterial used and the method of biomaterial processing to create such scaffolds are important because they influence cell behaviour, scaffold–cell interaction and ultimately tissue repair and quality of tissue reconstruction.[12–14]

Accordingly, we analysed the interaction of dermal fibroblasts and macrophages on a synthetic dermal matrix and on a biological dermal matrix, comparing their capacity to adhere, survive and proliferate within the three-dimensional structures and determined the balance between pro- and anti-inflammatory cytokine secretion. In this study, we aimed to evaluate how the presence of native collagen-elastin-based fibrillar network compares with the presence of polyurethane in cellular scaffold interactions and cytokine release profiles in response to the material the cells are grown on.

2 | EXPERIMENTAL PROCEDURES

2.1 | Materials

The biological wound matrix (MatriDerm®, abbreviation: BWM) was obtained from MedSkin Solutions Dr. Suwelack AG, Billerbeck, Germany. MatriDerm is composed of bovine collagen type I, III and V from bovine skin, supplemented with 2% elastin hydrolysate. It is manufactured by freeze-drying of acellular, purified dermal collagen to a

three-dimensional collagen sponge. The synthetic wound matrix (NovoSorb®, abbreviation: SWM) was acquired from PolyNovo Biomaterials PTY Ltd., Melbourne, Australia. NovoSorb is a bilayered dermal matrix made by a synthetic, biodegradable and biocompatible polyurethane matrix with a sealing layer. The sealing layer was removed prior to incubation with cells. Both matrixes are commercially available and are actively clinically used worldwide. Rabbit monoclonal antibody against collagen I (ab138492), rabbit polyclonal antibody against collagen III (ab7778), rabbit polyclonal antibody against collagen V (ab7046), rabbit polyclonal antibody against TGF-β1 (ab50038), rabbit polyclonal antibody against IL-10 (ab217941), rabbit polyclonal antibody against IL1-β (ab2105), rabbit polyclonal antibody against IL-6 (ab507) and rabbit polyclonal antibody against TNF-α (ab6671) were purchased from Abcam PLC, Cambridge, UK. Resazurin sodium salt was purchased from Sigma-Aldrich (catalogue number 7017).

2.2 | Transmission electron microscopy (TEM)

For TEM analysis, samples were punched out to 5-mm-diameter discs and incubated in phosphate-buffered saline (PBS) for 15 min at 4°C for rehydration. They were then used stand-alone, or in cell binding experiments as described below, fixed with 2.5% glutaraldehyde in 0.1 M sodium cacodylate, pH 7.4 (cacodylate buffer), washed with cacodylate buffer, and stored at 4°C. Specimens were subsequently embedded in Epon 812 and cut into ultrathin sections on a Reichert Ultracut S ultramicrotome (Leica Microsystems, Wetzlar, Germany). They were examined at the Core Facility for Integrated Microscopy (CFIM, Panum Institute, Copenhagen, Denmark) in a Philips/FEI CM100 BioTWIN transmission electron microscope. Images were recorded with a side-mounted Olympus Veleta camera using the ITEM acquisitions software provided by the manufacturer.

2.3 | Scanning electron microscopy (SEM)

The ultrastructure of both matrices was analysed using SEM, that is, the 3-D matrix architecture. Punched-out samples were prepared as described above, then fixed with 2.5% glutaraldehyde in cacodylate buffer. They were washed with cacodylate buffer and dehydrated with an ascending ethanol series, as previously described.[15] Carbon dioxide was used for critical point drying of the specimens and absolute ethanol was used as an intermediate solvent. They were mounted on aluminium holders, sputtered with 30 nm palladium/gold and examined in a Philips/FEI XL 30 field emission scanning electron microscope (FESEM) operated at 5 kV accelerating voltage.

2.4 | Immunoelectron microscopy

The matrix architecture, as well as the cellular architecture and cytokine secretion of macrophages and fibroblasts on the two matrices was assessed by transmission immunoelectron microscopy, as previously described in detail.[16] In all instances, matrix samples, with or without prior incubation with cells, were subjected to chemical fixation and EM preparation after finished experiments and all matrices were treated in the same way. The following antibodies and dilutions were used for immunolabelling: rabbit monoclonal collagen I antibody (1:80 dilution), rabbit polyclonal collagen III antibody (1:40 dilution), rabbit polyclonal collagen V antibody (1:60 dilution), rabbit polyclonal TGF-β1 antibody (1:30 dilution), rabbit polyclonal IL-10 antibody (1:30 dilution), rabbit polyclonal IL1-β antibody (1:80 dilution), rabbit polyclonal IL-6 antibody (1:60 dilution) and rabbit polyclonal TNF-α antibody (1:30 dilution). Specimens were examined in a Philips/FEI CM 100 TWIN transmission electron microscope, as described above.

2.5 | Cells and culture conditions

Adult human dermal fibroblasts ([HDFs], C0135C, Gibco) were purchased from Thermo Fisher Scientific, Waltham, USA. Cryopreserved cells were thawed according to the manufacturer's protocol and seeded into three 75-mL tissue culture flasks for expansion, each containing 15 mL of cellular growth medium consisting of Dulbecco's modified eagle medium (D-MEM) with 100 mM sodium pyruvate (PAA Laboratories, Pasching, Austria), supplemented with 10% fetal bovine serum (FBS) (PAA Laboratories, Pasching, Austria) and 2 mM L-glutamine (Invitrogen, Carlsbad, USA). Medium was changed every day and substituted with additional rhEGF at a final dilution of 1:1000. The cells were incubated for 7 days until they reached 80%–90% confluency. The cells were harvested by trypsinization (TrypLETM Select (1x), Life Technologies Corporation, Carlsbad, USA) and transferred into freezing medium, containing 1% BSA (Sigma Aldrich, St. Louis, USA) and 10% DMSO (Sigma-Aldrich, St. Louis, USA). A total of 1 mL aliquots of the cell suspension were transferred into cryotubes. The cryotubes were transferred to the freezer at −80°C for 24 h and

stored in liquid nitrogen until further use. Monocytes were isolated from buffy coat blood by double gradient centrifugation. The buffy coat blood was obtained from the Skåne University Hospital, Lund. The first density gradient was performed using Ficoll solution (Sigma-Aldrich) to separate mononuclear cells (460 g for 45 min). The iso-osmotic Percoll solution (Sigma-Aldrich) was used for the second-density gradient to isolate monocytes from peripheral blood mononuclear cells (800 g for 20 min at room temperature). Isolated monocytes were cultured in suspension culture plates in RPMI 1640 medium (Thermo Fisher) supplemented with 10% fetal calf serum, 1.5 mM NEAA, 2 mM l-glutamine, 1 mM sodium pyruvate, 0.05 mM β-mercaptoethanol, 1% penicillin–streptomycin, 10 ng/mL hM-CSF and 10 ng/mL hIL3 (all Peprotech) at 37 deg. and 5% CO_2. After 7 days, the cells were cultured in 10 ng/mL hM-CSF for further 5–7 days.

2.6 | Cell seeding of matrices

HDFs were gently thawed and counted in a haemocytometer using trypan blue (Fisher Scientific, Waltham, USA) to estimate the number of live/dead cells. Cells were suspended in a final cell concentration of 0.5×10^6 viable cells/mL. A total of 20 μL cell solution, corresponding to 10 000 cells, was added on top of punched-out wound matrix samples (5 mm punches), followed by incubation at 37°C at 5% CO_2 for multiple time points (15, 30, 60, 180 min in primary adhesion experiments, respectively, and 0, 24, 48, 96 h in proliferation experiments, respectively). In order to compensate for the differences in BWM and SWM to act as nutrient source for the cells, cell medium was replaced every other day. At each time point, cell medium was removed and the cell-seeded constructs were gently washed twice with PBS. The cell-seeded constructs were then fixed with 4% formaldehyde in PBS, followed by incubation at 4°C for 20 min. Finally, the cell-seeded constructs were rinsed three times in PBS and stored in 3 mL PBS until further evaluation.

2.7 | Cell attachment and distribution

Initial cell adherence (fibroblasts and macrophages) to the matrices was measured during 15, 30, 60 and 120 min by SEM, that is, cell density (cells/mm^2) and cell morphology (cell area, elongation and circularity). The characteristics of fibroblast and macrophage survival and distribution on the matrices were evaluated during 0, 1, 2 and 4 days by SEM, that is, cell density (cells/mm^2) and elongation (length/width). In order to determine the extent of cell surface area, elongation and circularity on different wound matrices, 50 images of each sample were randomly captured on 50 different locations, using the electron microscope's imaging software, allowing 300 cells per group to be evaluated. Cell surface area was defined by the product measured between the longest and shortest cell radius, multiplied by π. Cell elongation was measured as the quotient of the longest possible line perpendicular to each cell, and the longest possible line along the longitudinal axis of the cell. Cell circularity was determined as the quotient between cell surface area and cell perimeter, multiplied by 4π.

2.8 | Cell metabolism assay

Metabolic activity and proliferation of living cells were measured on the cell-seeded constructs (5 mm punches, 10 000 cells/punch) at 0, 24, 48 and 96 h. Cell-seeded constructs were incubated at 37°C and 5% CO_2, medium was replaced every other day. After each incubation time point, cell medium was removed and the cells were gently washed twice with PBS. 24-well plates were prepared by adding 500 μL medium, and the cell seeded constructs were transferred to the prepared 24-wells using a sterile forceps. Resazurin working solution (0.15%) was prepared by weighing 0.3 g Resazurin sodium salt dissolved in 200 mL PBS and sterile filtered. A total of 100 μL Resazurin working solution was added to all wells. Plates were incubated in a moisture chamber in a cell incubator for 4 hours at 37°C and 5% CO_2. A total of 100 μL medium were transferred from each well in duplicate to 96-well plates (black with transparent bottom). Subsequently, fluorescence at 555 nm excitation and 585 nm emission wavelengths was measured on a Spectramax i3x plate reader within 30 min.

2.9 | Cytokine analysis

Secretion of pro-inflammatory cytokines (interleukins [IL-1β, IL-6], tumour-necrosis factor-alpha [TNF-α]) and anti-inflammatory cytokines (transforming growth factor beta [TGF-β1], interleukin [IL-10]) by fibroblasts and macrophages on the matrices were assessed by two independent researchers during 1, 2 and 4 days by immunogold-TEM. These cytokines were chosen as they represent important players in early onset of wound healing. Electron micrographs were acquired in the electron microscope's iTEM software and gold particles were manually measured in Photoshop CS6.

2.10 | Statistical analysis

Student's t test for paired data was performed to determine statistical significance. Values were expressed as means ± standard error bars in the histograms. Statistical significances are expressed as n.s. ($p \geq 0.05$); * ($p \leq 0.05$); ** ($p \leq 0.01$); *** ($p \leq 0.005$).

3 | RESULTS

3.1 | Structural electron microscopic assessment of SWM and BWM

Using an electron microscopy approach by high-resolution field emission scanning electron microscopy (FESEM), we found that SWM was 100% amorphous in SEM images (Figure 1, left panel). In contrast, BWM exhibited a dermis-like collagen structure (Figure 1, right panel) with distinct pores (Figure 1B) and cross-striated collagen fibril bundles (Figure 1C).

3.2 | Cell adherence and distribution on SWM and BWM

3.2.1 | Morphological observations

The ability to provide versatile cell attachment sites is a key characteristic of wound matrices to provide optimal and efficient wound healing properties. Cell numbers represent the ability of cells to survive and proliferate on the matrix. Also, the way a given wound matrix interacts with cells in a beneficial way is represented by cell

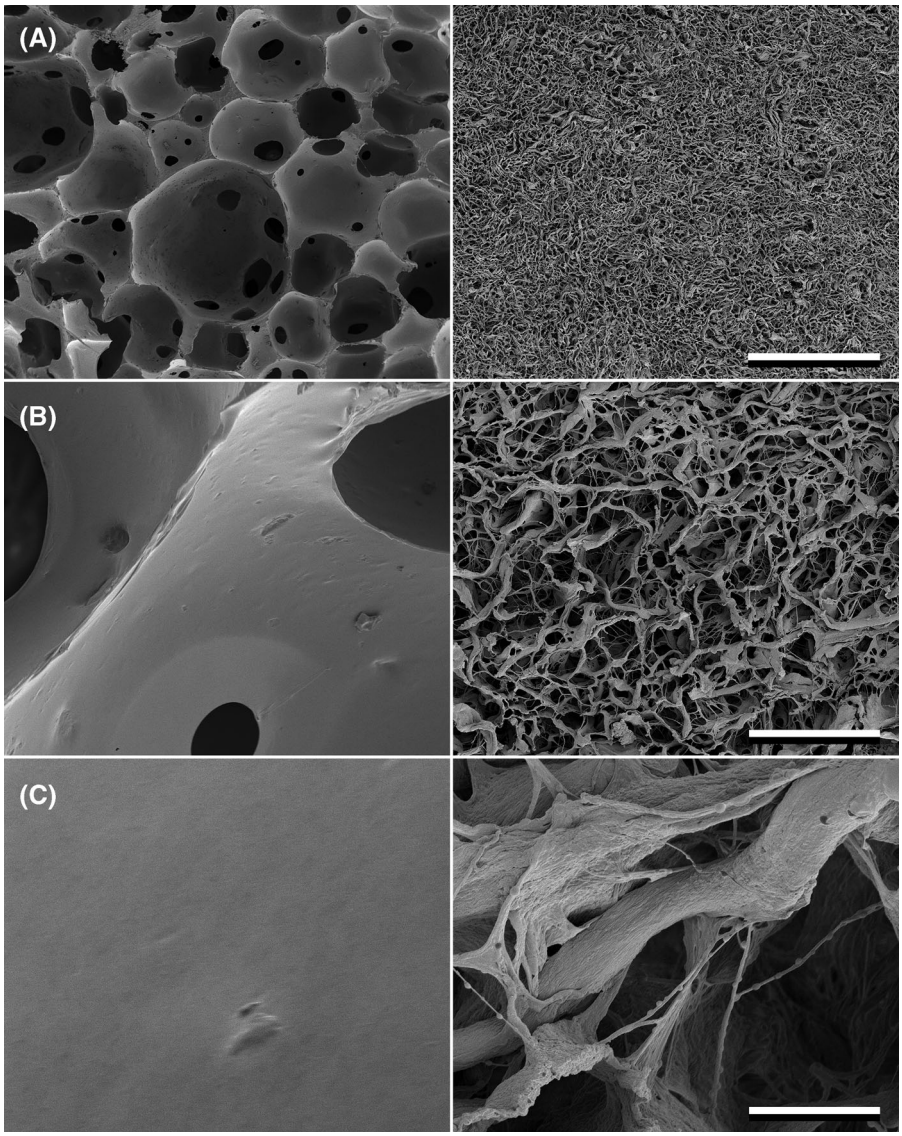

FIGURE 1 Ultrastructure of BWM and SWM as visualized by field emission scanning electron microscopy (FESEM). Specimens of SWM (A–C, left panel) were prepared for FESEM and compared with BWM (A–C, right panel) at different magnifications. Note the appearance of extended fibrillar collagen networks, interspaced by 20–80 μm pores in BWM (visible in B, C, right panel) and an abundance of large pores and amorphous sheets in SWM, rendering this material a Swiss cheese-like appearance (right panel). At higher magnification, bundles with cross-striated collagen fibrils are visible in BWM (C, right panel), whereas SWM appears amorphous (C, left panel). The scale bars represent 1 mm (A), 100 μm (B) and 10 μm (C).

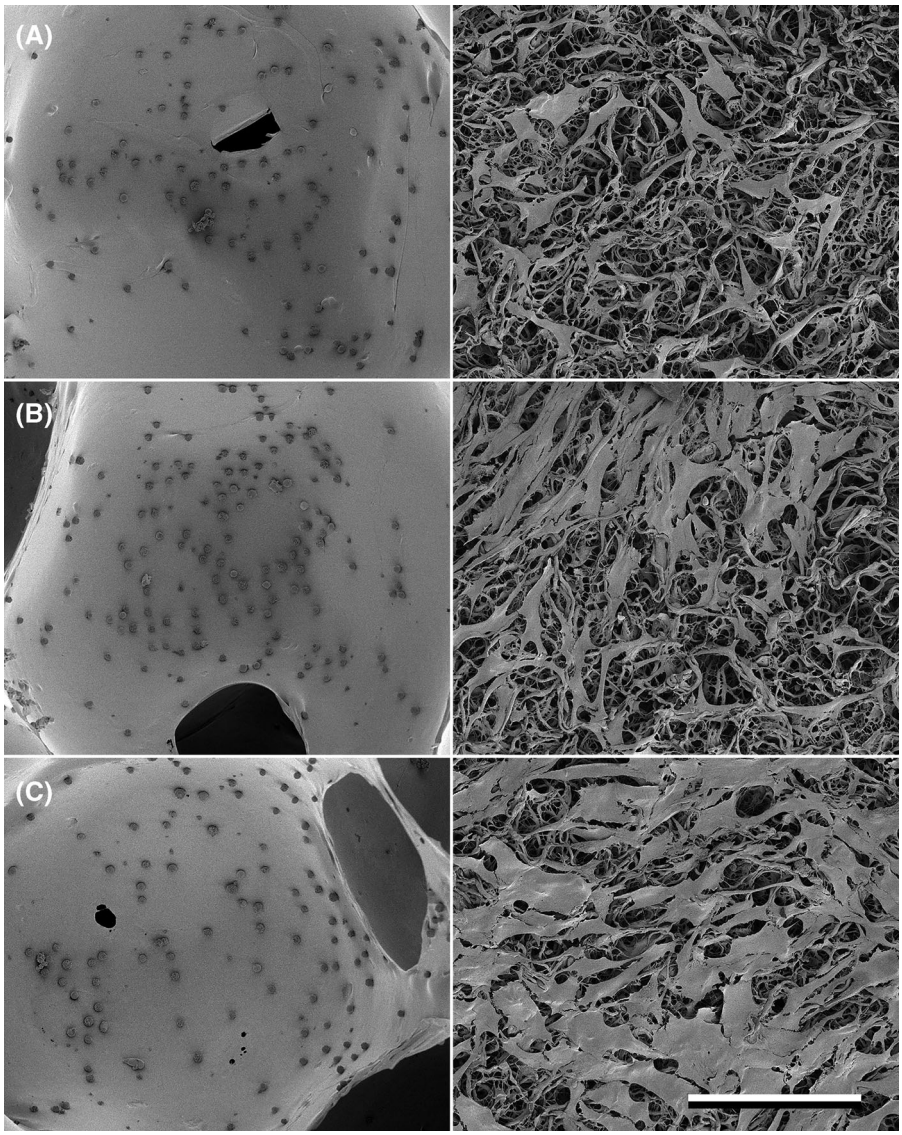

FIGURE 2 Characteristics of cell adherence and growth on BWM and SWM as visualized by FESEM at low magnification. SWM (left panel) and BWM (right panel) were incubated with human dermal fibroblasts for 24 h (A), 48 h (B) or 96 h (C). Fibroblasts on SWM do neither adhere nor proliferate well at all time points and are visualized as dark round dots (A–C, left panel). In contrast, fibroblasts adhere firmly to the native collagen fibrils in BWM, exhibit an elongated architecture and proliferate to form large cellular sheets (A–C, right panel). Similar results were obtained for macrophages on SWM and BWM (not shown). The scale bar represents 200 μm.

architecture parameters such as elongation, area and circularity. Therefore, in this work, these parameters were measured to assess the behaviour and morphology of the cells in response to the environment provided by BWM and SWM. These parameters have significant biological implications, particularly in relation to wound healing, where cell elongation reflects active movement and motility on the matrix. The area covered by a cell indicates how well a cell interacts with and firmly adheres to the matrix, which is beneficial for the wound healing process. Likewise, a surface that promotes cell migration may result in lower circularity values, with cells elongating as they move across the surface. To compare cell attachment sites of wound matrices, HDFs and macrophages were seeded onto SWM and BWM for 0, 24, 48 and 96 h. Figure 2 depicts representative examples of HDF adherence to and interaction with both materials. Specimens were then visualized and analysed by high-resolution FESEM. At higher magnification, large numbers of fibroblasts were observed in firm adhesion to collagen fibrils in BWM (Figure 3D–F), exhibiting an increasingly elongated cell architecture over the 96-h incubation. Initially, the fibroblasts were observed to have settled onto the collagen fibrils at 24-h time point (Figure 3D, arrowheads) and the plasma membrane became visibly in intimate contact with the collagen fibrils at 48-h time point (Figure 3E, arrowheads). After 96 h, fibroblasts in the process of depositing newly synthesized fibrillar extracellular matrix onto the BWM collagen framework were frequently observed. This extracellular matrix appeared as fine, spider web-like meshes on top of the thick fibre bundles of BWM (Figure 3F, arrowheads). In addition, such newly synthesized meshes were recovered from the cell culture medium of BWM at 96-h time points. They were collected and visualized by electron microscopy, where

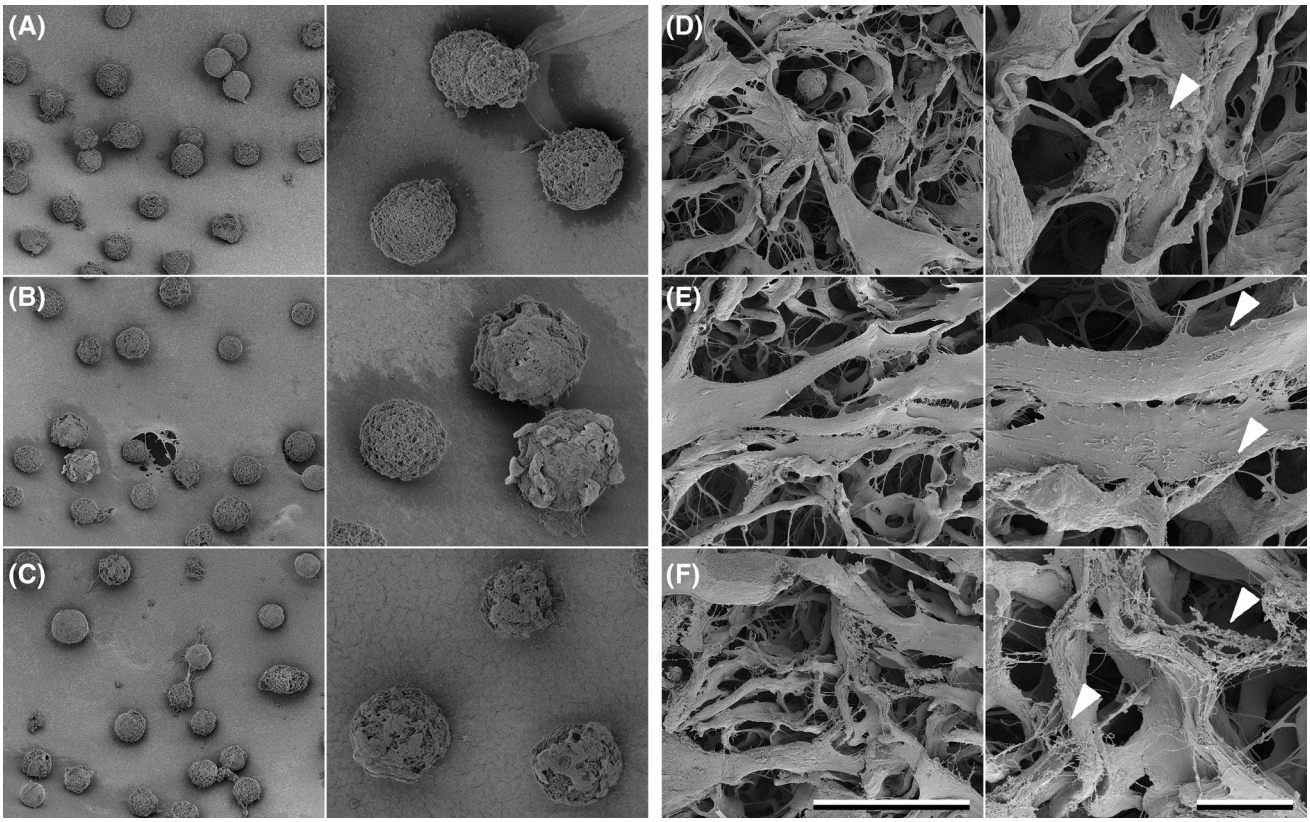

FIGURE 3 Characteristics of cell adherence and growth on BWM and SWM as visualized by FESEM at high magnification. SWM (A–C, left panel; intermediate magnification, right panel; high magnification) and BWM (D–F, left panel; intermediate magnification, right panel; high magnification) were incubated with human dermal fibroblasts for 24 h (A, D), 48 h (B, E) or 96 h (C, F). Fibroblasts on SWM exhibit a round structure at all time points (A–C). In contrast, fibroblasts adhere rapidly to the native collagen fibrils in BWM (D), spread into elongated structure along the BWM collagen fibrils (E) and deposit newly synthesized fibrillar extracellular material onto the BWM collagen scaffold (F). Note that cells presented in the right panel do not in all cases represent magnifications of cells from the left panel. The scale bars represent 50 μm (left panels) and 10 μm (right panels), respectively.

cross-striated collagen fibrils became visible (Suppl. Figure 1A). No such collagen fibrils were observed in cell culture supernatants from SWM (Suppl. Figure 1B). In addition, extended filopodia formation making cell–cell and cell–substrate contacts were observed at time points 48 and 96 h (Figure 3E, arrowheads). Fibroblasts deposited on SWM were predominantly observed to be of circular shape at all time points of incubation (Figure 2, left panel, Figure 3A–C). They were not observed to produce new extracellular structures after elongated incubation time points and showed no attachment to the SWM matrix (Figure 3C). Similar observations were made for macrophages. On BWM, the cells settled onto the collagen fibrils within 24 h and remained firmly attached throughout the experiment. However, they did not spread and proliferate in the same way as fibroblasts. On SWM, the macrophages remained round throughout all time points and exhibited the same appearance as the fibroblasts.

3.2.2 | Quantification of cell adherence and distribution

Initial fibroblast adherence during the first 120 minutes was about twice as much on BWM than on the SWM (Figure 4, upper panel). Similarly fibroblasts seeded onto BWM demonstrated a higher cell survival and proliferation during 96-h long-term incubations (Figure 4, lower panel), with a fourfold increase compared with fibroblasts seeded onto SWM by 96 h. The macrophages exhibited a somewhat different kinetics, where initial adhesion to BWM was complete after 24 h and no further proliferation was observed. Macrophages seeded onto SWM demonstrated initial adherence complete at 24 h and no further proliferation was observed. Significantly, the fibroblasts and macrophages seeded on SWM were completely circular at all analysed time points, with minimal contact to the substrate and covering a minimal surface area (500 vs. 600 cells/cm^2 at the last time point) (Figure 5).

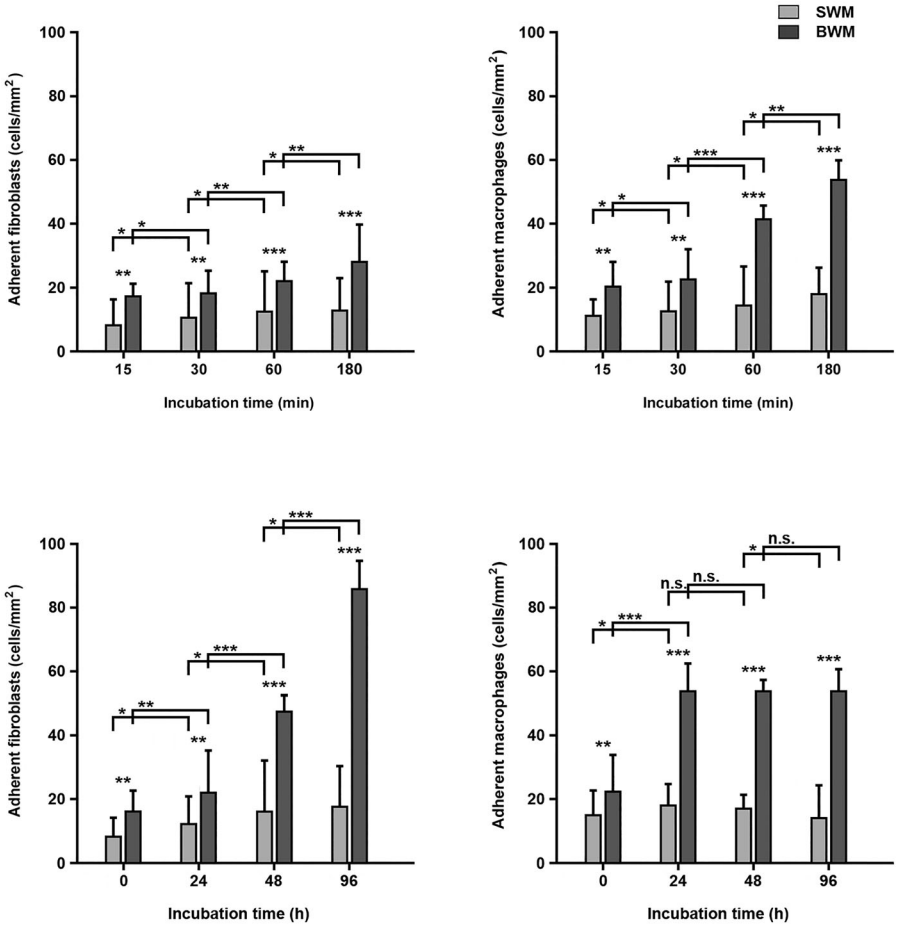

FIGURE 4 Quantitative evaluation of fibroblast and macrophage adherence to BWM and SWM. SWM and BWM specimens were incubated with fibroblasts and macrophages for 15, 30, 60 and 180 min (upper panel), or 0, 24, 48 and 96 h (lower panel). Adhered cells were identified and counted by electron microscopy, as shown in Figure 3. In each case, about 100 randomly selected electron micrographs were evaluated. Staples are given as means med SD error bars from three different experiments.

3.3 | Cytokine analysis

Cytokine release was measured on fibroblasts and macrophages seeded onto BWM and SWM at 0, 24, 48 and 96 h, using immune TEM with gold-labelled antibodies against pro- and anti-inflammatory cytokines relevant in the wound healing process (Figure 6). Overall, an increase in pro-inflammatory cytokines (i.e., IL-1β, IL-6, TNF-α) and a decrease in anti-inflammatory cytokines (i.e., TGF-β1, IL-10) were observed in cells seeded on SWM as compared with cells seeded on BWM (Figure 7). After 96 h, the increase of pro-inflammatory cytokines on BWM as compared with SWM was as follows: IL-1β: about 40%; IL-6: about 30%; TNF-α: about 50%. Accordingly, the increase of anti-inflammatory cytokines on BWM as compared with SWM was as follows: TGF-β1 (fibroblasts): some 4.3-fold; TGF-β1 (macrophages): some 4.75-fold; IL-10: some 4-fold.

3.4 | Metabolic activity and proliferation of cells

Numbers of living fibroblasts and macrophages were measured by the number of metabolically active cells at each time point up to 96 h (Figure 8). On BWM, the number of metabolically active and proliferative fibroblasts increased significantly over time and the number of metabolically active and proliferative macrophages remained constant after 24 h. Both fibroblasts and macrophages seeded onto SWM demonstrated a decrease in metabolic activity and proliferation over time, with a reduction of 50% of these properties measured at 96 h, as compared with cell-seeded values at time point 0 h.

4 | DISCUSSION

Wound healing is a response of the body to injury and achieves wound closure and scar tissue maturation through the wound healing cascade; composed of the inflammatory, proliferative, remodelling and maturation phase. These processes are carefully coordinated in a reciprocal manner between extracellular matrix constituents, different cell types and their soluble mediators.[17] Hence, key steps of the wound healing process, such as haemostasis, inflammation and angiogenesis are regulated in close communication collagen and its compounds.[18] An optimal environment for cellular adherence, survival and

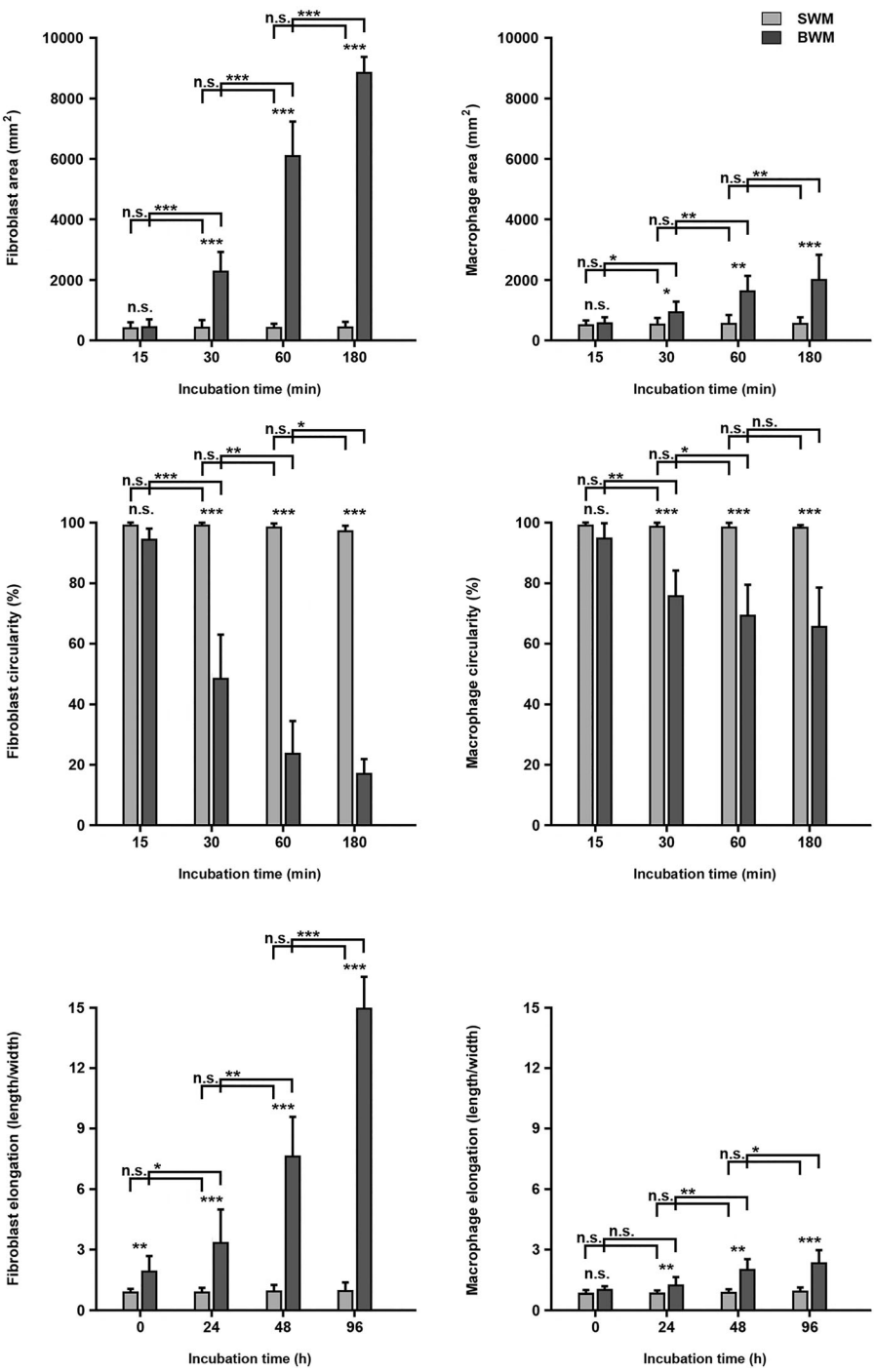

FIGURE 5 Quantitative evaluation of fibroblast and macrophage architecture on BWM and SWM. SWM and BWM specimens were incubated with fibroblasts and macrophages for 15, 30, 60 and 180 min (upper and middle panel), or 0, 24, 48 and 96 h (lower panel). Cellular parameters such as cell area (upper panel), cell circularity (middle panel) and cell elongation (lower panel) were determined on electron micrographs. In each case, about 100 cellular profiles were evaluated. Staples are given as means med SD error bars from three different experiments.

proliferation is achieved by replicating the structure and nature of a dermal matrix as close as possible to native skin. There are multiple ways to achieve native dermis resemblance and functionality. Biological biomaterial provides a native component as it is directly sourced from allogenic or xenogeneic hosts. However, processing of biological material and structuring of biological material are key for the performance of the resulting matrix. For example, allograft dermal matrices such as AlloDerm or GlyaDerm, sourced from human cadavers that have been decellularized, represent the closest natural structure to native human extracellular matrix; however, they are associated with the risk of disease transmission, rejection and immunogenic reactions due to the processes used to remove allogenic or xenogeneic cells. Incomplete removal of host cells from allogenic and xenogeneic material will result in poor outcomes.[19] To overcome these limitations, biological biomaterial can be sourced from a host, processed using different methods and tools such as lyophilization or cryopreservation, which is then reconstructed

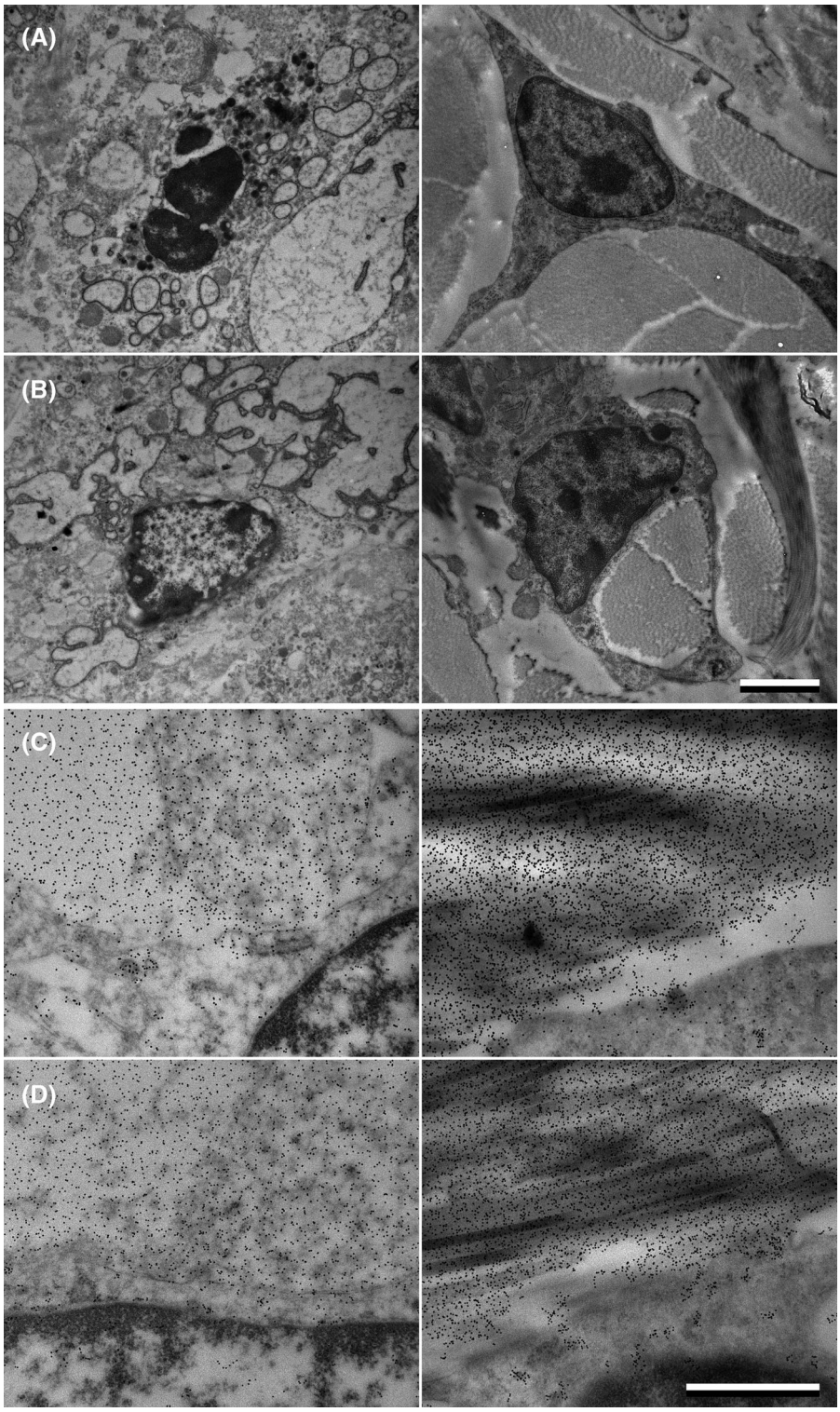

FIGURE 6 Immune TEM assessment of fibroblasts and macrophages on BWM and SWM. SWM (left panel) and BWM (right panel) were incubated for 96 h with fibroblasts (A) or macrophages (B) and subjected to ultrathin sectioning and TEM analysis. Note the intact cell architecture in the right panel, where cells are embedded in the collagen fibrils of BWM. This is opposed to the more deteriorated structures in the left panel, where nuclei and cytoplasm show signs of cell death. The scale bar represents 2 μm. (C, D), TEM and immunodetection of TGF-β1 secreted by fibroblasts (C) and macrophages (D). Immunodetection of IL-10, IL-1β, IL-6 and TNF-α was performed in the same way (not shown). The scale bar represents 1 μm.

into a dermal matrices, as MatriDerm, Integra and Pelnac. Furthermore, fine-tuning as pore size, porosity, tensile strength and other extracellular matrix parameters like substituting elastin as for MatriDerm can be performed. Alternatively, synthetic biomaterial has been developed to regulate characteristics such as pore size and porosity with high precision. Interestingly, the pore size of SWM, that is, 300–900 μm, is about 10 times beyond the physiological pore size for cells to interact and migrate.[20] Lacking in these dermal templates composed of synthetic material are the natural components of skin, unless these natural components can be replicated. Achieving a natural cellular interaction with an extracellular matrix, irrelevant of its biomaterial composition, and limiting unnecessary delay

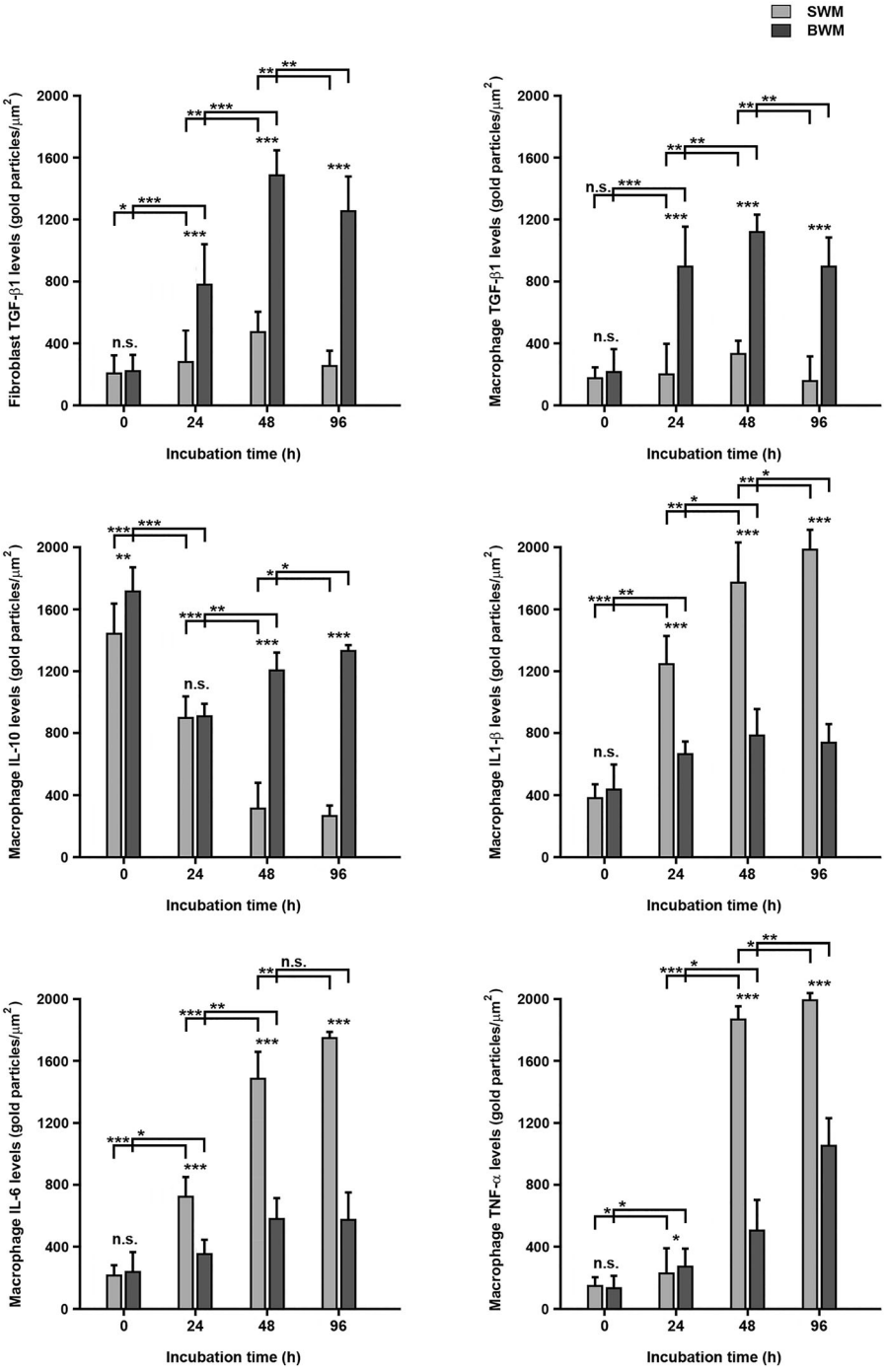

FIGURE 7 Quantitative evaluation of immune TEM analysis of cytokines secreted by fibroblasts and macrophages on BWM and SWM. BWM and SWM were incubated for 0, 24, 48 and 96 h with fibroblasts or macrophages, respectively, and subjected to ultrathin sectioning and immune TEM analysis. At each time point, the thin sections were analysed using old-labelled antibodies against TGF-β1, IL-10, IL-1β, IL-6 and TNF-α. The number of immunogold particles/μm^2 was determined in each case. Notably, the levels of pro-inflammatory cytokines increased, and the levels of anti-inflammatory cytokines decreased, over time on SWM, whereas the opposite effect was observed on BWM.

in wound healing, is the gold standard in wound healing matrix development.

Previously, Brown et al. conducted in vivo experiments to assess the influence of different ECM-based implants on wound regeneration. Wound sites with implants were compared with natural wound healing without implant. The results showed that natural wound matrices with a more native composition stimulated the formation of site-appropriate and functional new tissues that resembled a native restoration.[13,21,22] In another study, the beneficial effect of pure native collagen application to chronic wounds was shown, resulting in accelerated wound closure.[23] We have recently demonstrated that the innate properties of wound matrices with natural collagen scaffolds are beneficial for the proteolytic balance and cellular environment in the wound bed.[13,15] The present study supports our previous study, suggesting that collagen scaffolds are more beneficial than synthetic scaffolds for fibroblast and macrophage metabolic activity, proliferation and other cellular parameters in addition to regulating inflammatory response by modulating cytokine profiles of these cells, in an in vitro model.

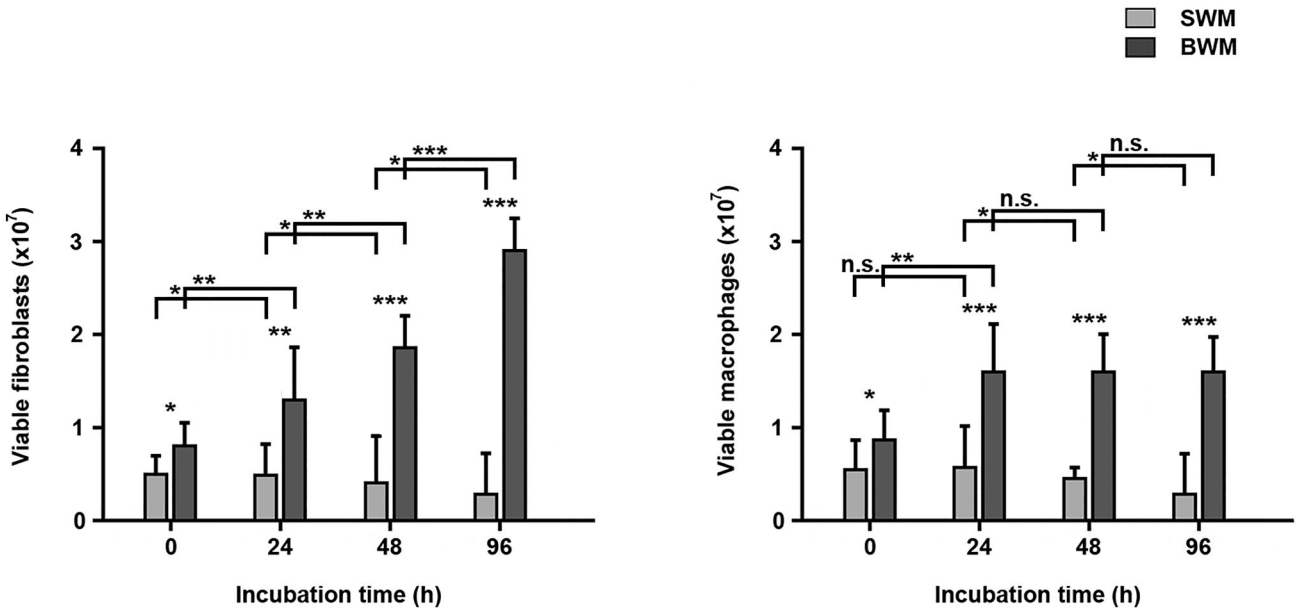

FIGURE 8 Cell viability on BWM and SWM. BWM and SWM were incubated with fibroblasts (left panel) or macrophages (right panel) for 0, 24, 48 and 96 h, respectively. At each time point, the biomaterials were assessed with Alamar Blue in order to analyse cell viability. Notably, cell viability increased (fibroblasts) or was maintained (macrophages) over time on BWM, whereas viability declined in all cases on SWM.

Over the past decades, a variety of matrix products have become well established for the management of wounds. These matrices provide active scaffolds with key elements that modulate inflammation, promote vascularization and re-epithelialization of the wound bed, and promote wound closure. Different matrices utilize different sources of materials and processing methodologies. Variations in these parameters impact the biochemical and structural properties of the scaffold in the final product and the biological response during wound healing.[24] Importantly, besides nativity of the collagen, porosity and pore size within the scaffold determine vital parameters of the invading cells, which, in turn, influence wound healing efficiency. In a recent study, Boekema et al. demonstrated that scaffolds with optimal pore sizes of 80–100 μm showed good results in wound healing after one-stage grafting. In contrast, scaffolds with larger average pore sizes resulted in more myofibroblasts and more foreign body giant cells.[25] This is in accordance with BWM having pore sizes in the range of 80–100 μm, whereas SWM has considerably larger pores. In this study, we found differences in all assessed parameters of cell scaffold interactions of fibroblasts and macrophages seeded onto BWM in comparison with SWM. The observed variations could be attributed to the presence of native collagen structures in BWM or the manufacturing process, resulting in optimal porosity and pore sizes. The manufacturing process of this specific BWM, MatriDerm, could also result in keeping native collagen structure of the bovine dermis raw material intact, contributing to favourable outcomes for fibroblast and macrophage adherence and proliferation in vitro. The fabrication of native collagen scaffolds has been shown to enhance their functionality by mimicking important natural dermis parameters and thus promote excellent tissue regeneration.[15,23,26–30] These studies also discuss the importance of the manufacturing process and the ability to save the nativeness of collagen is more important for the performance of collagen matrices than the animal source of collagen. The results are in accordance with our findings demonstrating that the collagen scaffold provides more desirable biomechanical, biochemical and cell biological properties than a synthetic scaffold in vitro.

Collagen matrices have been described as key components in the wound bed for the guidance of cell growth and migration during the proliferation and remodelling phase of the healing process.[31] Although there are many studies that demonstrate optimal characteristics of dermal templates to promote cell adherence and spreading, this study confirmed that cell adherence and natural spreading occurred more on the native collagen fibrils of BWM, as opposed to the pores of SWM. Historically, skin cells naturally adhere to the rigid, undulating synthetic flasks they are cultured and grown in, supporting the use of synthetic wound matrixes. However, in this study, we did not find the natural and well-established behaviour of cells in adherence and spreading to the SWM as we would observe in seeding into culture flasks, despite their

optimized pore size and porosity to support the adherence and distribution of cells into the scaffold. This might be due to the used polyurethane material and its processing, resulting in very large pore sizes, where adhesion and growth of invading cells are not supported.

Fibroblasts and macrophages are important cell types in the wound regeneration process with their unique capability to coordinate tissue repair (for recent reviews, see[32,33]). Importantly, during this process, they cross talk with other cell types in the wound microenvironment by secretion of pro- and anti-inflammatory cytokines and chemokines. Notably, the cytokine and chemokine profiles in the wound microenvironment orchestrate all wound healing stages.[34,35] As the wound healing phases progress, cytokine profiles are expected to shift from an overall pro-inflammatory to an anti-inflammatory state.[36,37] During incubation of cells on BWM, we observed elevated levels of the anti-inflammatory cytokines TGF-β1 and IL-10, and reduced levels of the anti-inflammatory cytokines IL-1β, IL-6 and TNF-α, which is in accordance with previous reports.[36,37] In contrast, the SWM surface promoted increased levels of IL-1β, IL-6 and TNF-α, and low levels of TGF-β1 and IL-10. This indicates that, on this material, cytokine production from adherent cells may have a prolonged influence on the normal inflammatory wound healing stages, creating an overall pro-inflammatory milieu on SWM. Although pro-inflammatory factors may be of benefit in an untreated non-healing wound and supports the under-stimulated or under-capacitated wound healing process in complex injuries, the long-term outcomes could potentially result in more scarring in wounds that need support and less over-stimulation.

The results discussed in this study suggest a more physiologic tissue regeneration occurring between cellular and biomaterial interface in BWM in comparison with SWM. However, it has to be considered that in vivo is a complex and dynamic interchange between different cell types, bodily fluids, microbial presence or contamination, pH and environmental changes, and mechanic agitation influencing the wound healing process and affecting the performance of dermal substitutes. The body's own capacity to repair is usually undamaged and wounds that often receive or need surgical intervention are those that are subject to poor wound healing associated with multiple factors such as smoking or co-morbidities like diabetes that impair the natural wound healing cascade. Specifically, when investigating the expression of inflammatory markers by cells in an in vitro environment, the environment is not a representation of the complexities found in vivo in both environmental and throughout the duration of wound healing, as the expression of inflammatory markers is a balancing act intertwined with the phases of wound healing. Therefore, it will be relevant to elucidate further the influence of in vivo wound healing environments on the interplay of dermal templates and different cell types involved in the wound healing process.

In summary, this study found that dermal fibroblast and macrophage proliferation, adherence and distribution were more favourable on BWM than SWM. The adhered cells on BWM exhibited a balanced secretion of different pro- and anti-inflammatory cytokines, in contrast to SWM. Although in vitro work, these results suggest the natural collagen fibres in BWM support a regenerative approach of wound healing and further investigations into optimal wound environments for BWM and SWM should be sought.

ACKNOWLEDGEMENTS

The matrix Matriderm® was supplied by Suwelack Skin & Health Care AG, Billerbeck, Germany. Writing and editorial assistance was provided by Deborah Nock (Medical WriteAway, Norwich, UK), funded by MedSkin Solutions Dr. Suwelack AG, Germany. We are grateful to the staff in the Microscopy Facility at the Department of Biology, Lund University, and the Core Facility for Integrated Microscopy (CFIM), Panum Institute, University of Copenhagen, for providing highly innovative environments for electron microscopy. We thank Ola Gustafsson (Microscopy Facility) for skillful work, and Klaus Qvortrup (CFIM) for practical help with electron microscopy.

FUNDING INFORMATION

The services of the medical writer (Deborah Nock) and electron microscopy services were funded by MedSkin Solutions Dr. Suwelack AG, Germany, who otherwise had no other role in this research.

CONFLICT OF INTEREST STATEMENT

The author declares no conflicts of interest.

DATA AVAILABILITY STATEMENT

Data available on request from the authors.

ORCID

Matthias Mörgelin https://orcid.org/0000-0002-6212-6990

REFERENCES

1. Wilkinson HN, Hardman MJ. Wound healing: cellular mechanisms and pathological outcomes. *Open Biol*. 2020;10(9):200223.
2. Zhou H, You C, Wang X, et al. The progress and challenges for dermal regeneration in tissue engineering. *J Biomed Mater Res A*. 2017;105:1208-1218.
3. Gurtner GC, Werner S, Barrandon Y, Longaker MT. Wound repair and regeneration. *Nature*. 2008;453:314-321.
4. Shah JMY, Omar E, Pai DR, Sood S. Cellular events and biomarkers of wound healing. *Indian J Plast Surg*. 2012;45:220-228.

5. Wound healing: an overview. Broughton G 2nd, Janis JE, Attinger CE. *Plast Reconstr Surg*. 2006;117(7 Suppl):1e-S-32e-S.
6. Rodríguez-Rodríguez N, Martínez-Jiménez I, García-Ojalvo A, et al. Wound chronicity, impaired immunity and infection in diabetic patients. *MEDICC Rev*. 2021;24:44-58.
7. Zhao R, Liang H, Clarke E, Jackson C, Xue M. Inflammation in chronic wounds. *Int J Mol Sci*. 2016;17:2085.
8. Li M, Hou Q, Zhong L, Zhao Y, Fu X. Macrophage related chronic inflammation in non-healing wounds. *Front Immunol*. 2021;12:681710.
9. Wall IB, Moseley R, Baird DM, et al. Fibroblast dysfunction is a key factor in the non-healing of chronic venous leg ulcers. *J Invest Dermatol*. 2008;128:2526-2540.
10. Lindholm C, Searle R. Wound management for the 21st century: combining effectiveness and efficiency. *Int Wound J*. 2016;13 Suppl 2(Suppl 2):5-15.
11. Pidgeon TS, Hollins AW, Mithani SK, Klifto CS. Dermal regenerative templates in Orthopaedic surgery. *J Am Acad Orthop Surg*. 2023;31(7):326-333.
12. Shpichka A, Butnaru D, Bezrukov EA, et al. Skin tissue regeneration for burn injury. *Stem Cell Res Ther*. 2019;10(1):94.
13. Dill V, Mörgelin M. Biological dermal templates with native collagen scaffolds provide guiding ridges for invading cells and may promote structured dermal wound healing. *Int Wound J*. 2020;17(3):618-630.
14. Varela P, Sartori S, Viebahn R, Salber J, Ciardelli G. Macrophage immunomodulation: an indispensable tool to evaluate the performance of wound dressing biomaterials. *J Appl Biomat Funct Mat*. 2019;17(1):2280800019830355.
15. Tati R, Nordin S, Abdillahi SM, Mörgelin M. Biological wound matrices with native dermis-like collagen efficiently modulate protease activity. *J Wound Care*. 2018;27:199-209.
16. Baschong W, Wrigley NG. Small colloidal gold conjugated to fab fragments or to immunoglobulin G as high-resolution labels for electron microscopy: a technical overview. *J Electron Microsc Tech*. 1990;14:313-323.
17. Almadani YH, Vorstenbosch J, Davison PG, Murphy AM. Wound healing: a comprehensive review. *Semin Plast Surg*. 2021;35:141-144.
18. Mathew-Steiner SS, Roy S, Sen CK. Collagen in wound healing. *Bioengineering (Basel)*. 2021;8:63.
19. Zhang X, Chen X, Hong H, Hu R, Liu J, Liu C. Decellularized extracellular matrix scaffolds: recent trends and emerging strategies in tissue engineering. *Bioact Mater*. 2022;10:15-31.
20. Stefanelli VL, Mintz B, Gandhi A, Smith J. Design matters: a comparison of natural versus synthetic skin substitutes across benchtop and porcine wound healing metrics: an experimental study. *Health Sci Rep*. 2023;6(8):e1462.
21. Brown BN, Chung WL, Pavlick M, et al. Extracellular matrix as an inductive template for temporomandibular joint meniscus reconstruction: a pilot study. *J Oral Maxillofac Surg*. 2011;69:e488-e505.
22. Brown BN, Chung WL, Almarza AJ, et al. Inductive, scaffold-based, regenerative medicine approach to reconstruction of the temporomandibular joint disk. *J Oral Maxillofac Surg*. 2012;70:2656-2668.
23. Wahab N, Roman M, Chakravarthy D, Luttrell T. The use of a pure native collagen dressing for wound bed preparation prior to use of a living bi-layered skin substitute. *J Am Coll Clin Wound Spec*. 2014;6:2-8.
24. Hughes OB, Rakosi A, Macquhae F, Herskovitz I, Fox JD, Kirsner RS. A review of cellular and acellular matrix products: indications, techniques, and outcomes. *Plast Reconstr Surg*. 2016;138:138S-147S.
25. Boekema BKHL, Vlig M, Damink LO, et al. Effect of pore size and cross-linking of a novel collagen-elastin dermal substitute on wound healing. *J Mater Sci Mater Med*. 2014;25:423-433.
26. Brett D. A review of collagen and collagen-based wound dressings. *Wounds*. 2008;20:347-356.
27. de Francesco F, de Francesco M, Riccio M. Safety and efficacy of collagen-based biological dressings in the management of chronic superficial skin wounds in non-complex trauma: a post-marketing surveillance study. *Trauma Care*. 2021;1:195-205.
28. Böhm S, Strauss C, Stoiber S, Kasper C, Charwat V. Impact of source and manufacturing of collagen matrices on fibroblast cell growth and platelet aggregation. *Materials (Basel)*. 2017;10:1086.
29. Killat J, Reimers K, Choi CY, Jahn S, Vogt PM, Radtke C. Cultivation of keratinocytes and fibroblasts in a three-dimensional bovine collagen-elastin matrix (MatriDerm®) and application for full thickness wound coverage in vivo. *Int J Mol Sci*. 2013;14:14460-14474.
30. Gabler C, Spohn J, Tischer T, Bader R. Biomechanical, biochemical, and cell biological evaluation of different collagen scaffolds for tendon augmentation. *Biomed Res Int*. 2018;2018:7246716.
31. Doillon CJ, Silver FH, Olson RM, Kamath CY, Berg RA. Fibroblast and epidermal cell-type I collagen interactions: cell culture and human studies. *Scanning Microsc*. 1988;2:985-992.
32. Talbott HE, Mascharak S, Griffin M, Wan DC, Longaker MT. Wound healing, fibroblast heterogeneity, and fibrosis. *Cell Stem Cell*. 2022;29:1161-1180.
33. Kim SY, Nair MG. Macrophages in wound healing: activation and plasticity. *Immunol Cell Biol*. 2019;97:258-267.
34. Barrientos S, Stojadinovic O, Golinko MS, Brem H, Tomic-Canic M. PERSPECTIVE ARTICLE: growth factors and cytokines in wound healing. *Wound Repair Regen*. 2008;16:585-601.
35. Strang H, Kaul A, Parikh U, et al. Chapter 11 – role of cytokines and chemokines in wound healing. *Wound Healing, Tissue Repair, and Regeneration in Diabetes*. Academic Press; 2020:197-235.
36. Jones JA, Chang DT, Meyerson H, et al. Proteomic analysis and quantification of cytokines and chemokines from biomaterial surface-adherent macrophages and foreign body giant cells. *J Biomed Mater Res A*. 2007;83:585-596.
37. Rodriguez A, Meyerson H, Anderson JM. Quantitative in vivo cytokine analysis at synthetic biomaterial implant sites. *J Biomed Mater Res A*. 2009;89:152-159. doi:10.1002/jbm.a.31939

SUPPORTING INFORMATION

Additional supporting information can be found online in the Supporting Information section at the end of this article.

How to cite this article: Hong JP, Maitz J, Mörgelin M. Comparison of cell-scaffold interactions in a biological and a synthetic wound matrix. *Int Wound J*. 2025;22(1):e70108. doi:10.1111/iwj.70108